

1 **Increased pCO₂ and temperature reveal ecotypic differences in growth and**
2 **photosynthetic performance of temperate and Arctic populations of *Saccharina latissima***

3 **Mark Olischläger, Concepción Iñiguez, Kristina Koch, Christian Wiencke, Francisco**
4 **Javier López Gordillo**

5 **Abstract**

6 Previous research demonstrated that warming and ocean acidification (OA) affect the biochemical
7 composition of Arctic (Spitsbergen; SP) and cold-temperate (Helgoland; HL) *Saccharina latissima*
8 differently, suggesting ecotypic differentiation. The present study analyses the responses to different
9 pCO₂ (380, 800, 1500 µatm pCO₂) and temperature levels (SP population: 4°C, 10°C; HL population:
10 10°C, 17°C) on the photophysiology (O₂ production, pigment composition, D1-protein content) and
11 carbon assimilation (Rubisco content, carbon concentrating mechanisms (CCMs), growth rate) of both
12 ecotypes. Elevated temperatures stimulated O₂ production in both populations, and also led to an
13 increase in pigment content and a deactivation of CCMs, as indicated by ¹³C isotopic discrimination of
14 algal biomass (ε_p) in the HL population, which was not observed in SP thalli. Generally, pCO₂ effects
15 were less pronounced than temperature effects. High pCO₂ deactivated CCMs in both populations and
16 produced a decrease in the Rubisco content of HL thalli while it was unaltered in SP population. As a
17 result, the growth rate of the Arctic ecotype increased at elevated pCO₂ and higher temperatures and it
18 remained unchanged in the HL population. Ecotypic differentiation was revealed by a significantly
19 higher O₂ production rate and an increase in Chl *a*, Rubisco and D1-protein content in SP thalli, but a
20 lower growth rate, in comparison to the HL population. We conclude that both populations differ in
21 their sensitivity to changing temperatures and OA and that the Arctic population is more likely to
22 benefit from the upcoming environmental scenario than its Atlantic counterpart.

23 **Keywords**

24 Arctic · Carbon concentrating mechanisms · Kelp · Ocean acidification · Photosynthesis · Pigment ·
25 Seaweed

26 **Abbreviations**

27 CCM Carbon concentrating mechanism

28 DPS De-epoxidation state

29 DW Dry weight

30 ϵ_p Isotopic fractionation of organic carbon production

31 HL Helgoland

32 OA Ocean acidification

33 pCO_2 Partial pressure of CO_2

34 PS Photosystem

35 RGR Relative growth rate

36 ROS Reactive oxygen species

37 SP Spitsbergen

38 VAZ Xanthophyll cycle pigment pool

39

40

41

42 **Introduction**

43 The rise of atmospheric pCO₂ causes changes in the seawater carbonate system (SWCS), resulting in
44 an increase in CO₂, HCO₃⁻ and overall DIC, a decrease in CO₃²⁻ and a concomitantly lower pH. These
45 changes are known as ocean acidification (OA) (Riebesell et al. 2010). During the last decades, OA-
46 effects on marine algae got into the focus of marine research, revealing that the OA effects on
47 photoautotrophs are species-specific, bearing positive, negative and neutral responses to elevated
48 pCO₂ (e.g. Koch et al. 2013). It is becoming increasingly established that the outcome of OA-effects
49 on growth and photosynthesis are dependent on the interaction with other environmental constraints,
50 such as suboptimal temperatures, including global warming scenarios (Fu et al. 2007; Feng et al. 2008;
51 ; Olischläger and Wiencke 2013; Sarker et al. 2013) and limited phosphorous availability (Xu et al.
52 2010). In some algae OA-effects are enhanced at limiting light conditions (Rokitta and Rost 2012),
53 whereas other algae species are only sensitive towards OA at saturating light (Sarker et al. 2013) or
54 under replete nitrogen conditions (Gordillo et al. 2001).

55 The long-term adaptation of an algal population to its local environment results in ecotypic
56 differentiation possibly influencing also the response to OA. It was postulated that algae in cold seas
57 are less dependent on active carbon uptake, since cold polar waters generally contain high
58 concentrations of dissolved CO₂, which are considered as saturating for algal photosynthesis at low
59 temperatures (Raven et al. 2002). However, high activities of external carbonic anhydrases (eCAs)
60 were measured in all polar macroalgae tested (Gordillo et al. 2006), even in those lacking CCM such
61 as *Phycodryas rubens*, pointing to a demand of continuous supply of CO₂ to the cells. In most of the
62 analysed species, this high eCA activity was supposed to be involved in CCM operation, as suspected
63 from the ¹³C discrimination values obtained for polar seaweeds (Wiencke and Fischer 1990). For the
64 OA-sensitivity of each species the question whether or to which extent an alga operates an active
65 carbon concentrating mechanism (CCM) is considered to be crucial (Hepburn et al. 2011). Therefore,
66 if polar algae are CO₂-saturated at present it is reasonable to assume that they are rather insensitive
67 towards OA. On the other hand, if polar macroalgae need to express CCMs strongly, Arctic algae
68 might be particularly sensitive towards OA, since a higher environmental pCO₂ facilitates passive

69 diffusion from the surrounding seawater towards Rubisco, allowing a down-regulation of the energy
70 demanding CCM and a reallocation of the resources used (Raven et al. 2012). Furthermore, a future
71 scenario with higher environmental CO₂ can compensate a low temperature-induced CCM inefficiency
72 (Olischläger and Wiencke 2013), which might be particularly important for species growing at the
73 edge of their physiological temperature range of tolerance. Such species might be Arctic macroalgae,
74 since the present marine flora reinvaded the Arctic after the ice-melt of the last glaciation event, less
75 than 18000 years ago from the North Atlantic and North Pacific (Lüning 1990). The Arctic
76 populations derive from the cold-temperate zones of the North-Atlantic and many species still grow in
77 cold temperate and polar habitats (Lüning 1990). The low degree of endemism in the Arctic relative to
78 the Antarctic can be explained by this small time interval. Nevertheless, indices of an ecotypic
79 differentiation were already reported in relation to zoospore germination and biochemical composition
80 of the cold-temperate and polar kelp *Saccharina latissima* (Müller et al. 2008; Olischläger et al. 2014).
81 The latter species occurs in cold-temperate and in polar environments (Lüning 1990) and, therefore, it
82 is particularly relevant to perform a comparison between both populations regarding its OA-response,
83 tackling the question whether or not polar macroalgae populations are less susceptible towards OA
84 than their temperate counterparts.

85 It was observed that the photosynthetic response to cultivation at elevated pCO₂ is often neutral or
86 positive (Harley et al. 2012; Olischläger et al. 2012; Olischläger and Wiencke 2013; Sarker et al.
87 2013), whereas the Rubisco and protein contents are often down-regulated in response to cultivation at
88 elevated pCO₂ (Andría et al. 2001, Gordillo et al. 2001). Hence, at elevated pCO₂, an improved
89 photosynthetic performance can be achieved by the same amount of Rubisco and pigments, if Rubisco
90 was not saturated at actual CO₂ concentrations (the majority of algae from temperate areas, Raven and
91 Beardall 2003), resulting in a more efficient resource-use. For algae with CCMs, increased pCO₂ could
92 lead to an unchanged photosynthetic rate but an increased growth rate due to CCM down-regulation
93 (Gordillo et al. 2001), as CCM activity have associated an energy cost (Raven and Beardall 2016). In
94 either case, this indicates a decreased amount of energy demand at high pCO₂, which might trigger a
95 re-arrangement of the light harvesting complex, consisting in the elimination of pigment molecules
96 that are in excess and would not participate efficiently in the light capture. Thus, a decrease in pigment

97 content at high CO₂ has been frequently observed as part of the acclimation process (e.g. García-
98 Sanchez et al. 1994; Gordillo et al. 1999; Gordillo et al. 2001). The D1 protein is a key component of
99 PS II reaction center, so that a change in the number of PS II should be reflected also in the amount of
100 D1. However, this relation can be modified by different degradation and replacement rates during
101 photoinhibition (Segovia et al. 2015).

102 Clearly, the physiological response to elevated pCO₂ is also temperature dependent (Fu et al. 2008;
103 Olischläger and Wiencke 2013; Sarker et al. 2013). The reason for these findings might be that
104 photosynthetic light reactions are independent of temperature (Raven and Geider 1988), whereas the
105 enzymatic reactions involved in the photosynthesis and carbon acquisition are not (Raven and Geider
106 1988; Olischläger and Wiencke 2013). Hence, an effective avoidance of photoinhibition requires a
107 balance between excitation, in the light harvesting reactions and the enzymatic carbon acquisition and
108 assimilation. Therefore, the aim of the study was to link the effects of pCO₂ and temperature to light
109 harvesting, carbon acquisition and fixation. Furthermore, we compared the results from cold-temperate
110 and polar populations of *S. latissima* and tested if ecotypes differ in their response pattern to OA and
111 temperature.

112 The following hypotheses were tested: (i) Arctic and temperate populations of *S. latissima* show
113 ecotypic differentiation in their photophysiology and growth. (ii) Arctic and temperate populations of
114 *S. latissima* show different sensitivity to OA, with a less sensitive response of the Arctic population
115 towards OA in term of pigmentation, photosynthesis and growth. (iii) Pigmentation and Rubisco
116 content are down-regulated synchronously at elevated pCO₂ in both populations, and (iv) OA effects
117 are more pronounced at low temperatures in both populations.

118 **Material and methods**

119 **Algal material and experimental conditions**

120 As previously described by Olischläger et al. (2014), young vegetative sporophytes were raised from
121 polar and temperate *S. latissima* gametophytes (Spitsbergen; AWI-culture number: ♂-gametophytes
122 3123, ♀-gametophytes 3124; Helgoland, North Sea; AWI-culture number: ♂-gametophytes 3094, ♀-

123 gametophytes 3096). Male and female gametophytes from the two populations were mixed, carefully
124 fragmented with pestle and mortar and kept in dim white light ($15\text{-}20 \mu\text{mol photons m}^{-2} \text{s}^{-1}$) at 10°C
125 until experimental use. For the experiment, a photon fluence rate (PFR) of $70 \pm 10 \mu\text{mol photons m}^{-2} \text{s}^{-1}$
126 at the bottom and $120 \pm 10 \mu\text{mol photons m}^{-2} \text{s}^{-1}$ at the top of the beaker was adjusted, using a flat
127 head cosine corrected quantum sensor attached to a radiometer (Li-185-B, flat head quantum sensor;
128 LI-COR Biosciences, Lincoln, NE, USA). Fluorescent tubes were used as light source (OSRAM 58W
129 /965 Biolux, Munich, Germany).

130 The experiment was started by transferring $0.5 \pm 0.1 \text{ g}$ fresh weight of algae from the precultivation to
131 5 L beakers filled with filtered seawater (FSW; $0.2 \mu\text{m}$), enriched with unbuffered nutrients after
132 Provasoli (1968), including 2.0 mM NO_3^- and $0.05 \text{ mM PO}_4^{3-}$. Experimental beakers were aerated
133 continuously with artificial air (20% oxygen, 80% nitrogen) with a target pCO_2 of $380 \mu\text{atm}$, 800
134 μatm , or $1500 \mu\text{atm}$ generated by a gas mixing device (HTK GmbH, Hamburg, Germany).

135 Subsequently, these pCO_2 treatments are called ‘present’, ‘expected’ and ‘high’ pCO_2 . The media
136 were aerated with the different gas mixtures described above for 24 h prior to experimental use and
137 water was exchanged every 3-4 days. Thalli were moved continuously by aeration without tumbling.
138 The experiment lasted 18 days, and was performed in temperature-controlled rooms adjusted to 17°C
139 $\pm 1.5^\circ\text{C}$ and $10^\circ\text{C} \pm 1.5^\circ\text{C}$ for the Helgoland population and $10^\circ\text{C} \pm 1.5^\circ\text{C}$ and $4^\circ\text{C} \pm 1.5^\circ\text{C}$ for the
140 Spitsbergen population. 10°C is chosen for the examination of the ecotypic differentiation, since the
141 10°C isotherme in August is considered to be the boundary between the marine cold-temperate and the
142 Arctic zone (Lüning 1990) and the two populations could theoretically coexist in northern continental
143 Norway (Lüning 1990).

144 **Monitoring of the seawater carbonate system during the experiment**

145 The seawater carbonate system (SWCS), including the pCO_2 of the FSW was monitored as described
146 by Olischläger et al. (2014). The equilibrium constants for the dissociation of carbonic acid in
147 seawater from Millero et al. (2006), and for sulfuric acid the constants of Dickson (1990), were
148 applied in the calculations. The pH was monitored on a total scale, except for one measuring date in
149 SP 10°C -treatment, for which the pH was measured on the National Bureau of Standards (NBS)-Scale

150 due to a technical failure. The SWCS-calculations of this measurement date used the dissociation
151 constants for carbonic acid from Takahashi et al. (1982), which are recommended for the NBS-scale.
152 Detailed values of the measured characteristics of the SWCS are presented in this accompanying
153 publication (Olischläger et al. 2014).

154 **Pigment analysis**

155 Determination of pigment content was performed by a reversed phase HPLC. Algal samples were
156 lyophilized for 24 h and pulverized at 4 m s⁻¹ for 20 s in a high-speed benchtop homogenizer
157 (FastPrep[®]-24; MP Biomedicals, Solon, OH, USA). Pigments in the samples (approx. 30 mg dry
158 weight) were extracted in 1 mL of ice-cold 90% acetone for 24 h at -20°C in darkness. After
159 centrifugation (5 min, 4°C, 13000 g) and filtration through a 45 µm nylon syringe filter (Nalgene[®],
160 Nalge Nunc International, Rochester, NY, USA), HPLC analyses were performed on a LaChromElite[®]
161 system equipped with a chilled autosampler L-2200 and a DAD detector L-2450 (VWR-Hitachi
162 International GmbH, Darmstadt, Germany). A Spherisorb[®] ODS-2 column (25 cm x 4.6 mm, 5 µm
163 particle size; Waters, Milford, MA, USA) with a LiChropher[®] 100-RP-18 guard cartridge was used for
164 the separation of pigments, applying a gradient according to Wright et al. (1991). Peaks were detected
165 at 440 nm and identified as well as quantified by co-chromatography with standards for chl *a* and *c*₂,
166 fucoxanthin, β-carotene, violaxanthin, antheraxanthin and zeaxanthin (DHI Lab Products, Hørsholm,
167 Denmark) using the software EZChrom Elite ver. 3.1.3. (Agilent Technologies, Santa Clara, CA,
168 USA). Pigment contents were expressed as µg per mg dry weight.

169 Further, the de-epoxidation state (DPS) of the xanthophyll cycle pigments was calculated as follows:

$$170 \text{ DPS} = ([\text{Zea}] + 0.5 \times [\text{Ant}]) / \text{VAZ}$$

171 where Ant is antheraxanthin, Zea is zeaxanthin and VAZ is the xanthophyll cycle pigment pool (sum
172 of viola-, anthera- and zeaxanthin). The DPS represents the photoprotective state of the xanthophyll
173 cycle as ant- and zeaxanthin play an important role in the dissipation of excess excitation energy as
174 heat and thereby protecting the reaction centers against photoinhibition (Pfündel and Bilger 1994;
175 Colombo-Palotta et al. 2006).

176 **Rubisco and D1 protein quantification**

177 Protein extraction procedure was performed as explained by Olischlager et al. (2014). Proteins from
178 extracts and Rubisco standard were resolved by SDS-PAGE (Laemmli 1970) in Mini-Protean Tetra
179 Cell (Bio-Rad, Hercules, USA) at a constant voltage of 175 V during 60 min, using 12%
180 polyacrylamide in the resolving gel. All lanes were loaded with 50 µg protein.

181 The amount of Rubisco was estimated by Coomassie Brilliant Blue polyacrylamide gel staining
182 procedure (Neuhoff et al. 1988), using purified spinach Rubisco as standard (R-8000, Sigma-Aldrich,
183 St. Louis, MO, USA). Stained gels were photographed, and bands identified as Rubisco large subunits
184 were quantified with the Molecular Imaging Software (Eastman-Kodak, Rochester, NY, USA) based
185 on both size and intensity.

186 Changes in the relative amounts of D1 protein were detected by subsequent blotting after
187 electrophoresis using a D1-specific primary antibody (AS 01016 Chicken Anti PsbA, Agrisera,
188 Sweden) at 1:10000 dilution, and anti-chicken IgY-HRP conjugated (Abcam, Cambridge, United
189 Kingdom) as secondary antibody at 1:15000 dilution. The signal was detected by chemiluminescence
190 (ECL-Plus; GE Healthcare, Buckinghamshire, UK) using a KODAK Gel Logic 1500 Imaging System
191 (Eastman-Kodak, Rochester, NY, USA), and the relative intensity of cross-reactions was quantified as
192 above.

193 **Chlorophyll fluorescence**

194 After 14 days of treatment the effective quantum yield ($\Delta F/F_m'$) was quantified by measuring the
195 variable chlorophyll fluorescence of photosystem II (PSII), using a PAM-2100 (Walz-GmbH,
196 Effeltrich, Germany), following Maxwell and Johnson (2000). The saturation pulse lasted 800 ms and
197 had an irradiance of 8500 µmol photons m⁻² s⁻¹ (400-800 nm).

198 **Net photosynthesis**

199 Net photosynthesis was estimated by O₂ evolution after 15 and 16 days as described in Olischläger et
200 al. (2012), at an irradiance of 120 µmol m⁻² s⁻¹, at 17°C and 10°C for the HL population, and at 10°C

201 and at 4°C for the SP population. In order to obtain more information from this measurement, O₂
202 production rates were calculated with respect to DW, Chl *a* content and Rubisco content.

203 **Stable carbon isotopic determination**

204 The abundance of ¹³C relative to ¹²C in plant samples was determined by mass spectrometry using a
205 DELTA V Advantage (Thermo Electron Corporation, USA) Isotope Ratio Mass Spectrometer (IRMS)
206 connected to a Flash EA 1112 CNH analyser. The ¹³C isotopic discrimination in the algal samples
207 ($\delta^{13}\text{C}_{\text{alga}}$) was calculated as deviations from the ¹³C/¹²C ratio of the Pee-Dee Belemnite CaCO₃ (PDB).
208 Isotopic fractionation of organic carbon production (ϵ_p) was calculated from the $\delta^{13}\text{C}_{\text{alga}}$ value relative
209 to the isotopic composition of dissolved CO₂ ($\delta^{13}\text{C}_{\text{CO}_2}$) in the medium according to Freeman and
210 Hayes (1992):

$$211 \epsilon_p = (\delta^{13}\text{C}_{\text{CO}_2} - \delta^{13}\text{C}_{\text{alga}}) / (1 + (\delta^{13}\text{C}_{\text{alga}}/1000))$$

212 This correction of the $\delta^{13}\text{C}_{\text{alga}}$ with the $\delta^{13}\text{C}_{\text{CO}_2}$ was needed, since the CO₂ source used in the
213 experiment for the CO₂-enriched treatment came from previously fixed CO₂ which had already been
214 subjected to discrimination relative to CO₂ dissolved in seawater.

215 To determine the isotopic composition of dissolved inorganic carbon ($\delta^{13}\text{C}_{\text{DIC}}$), 20 ml of FSW from
216 each cylinder was filtered (Whatman GF/F) and stored at 2°C in dark in septum-sealed glass vials
217 without leaving a head-space until analysis. Measurements of $\delta^{13}\text{C}_{\text{DIC}}$ were taken with the same IRMS
218 connected to a GasBench II (Thermo Electron Corporation) system. The isotopic composition of
219 dissolved CO₂ ($\delta^{13}\text{C}_{\text{CO}_2}$) in the medium was calculated from $\delta^{13}\text{C}_{\text{DIC}}$, following a mass-balance
220 equation (Zeebe and Wolf-Gladrow 2001). Fractionation factors between CO₂ and HCO₃⁻ and
221 between HCO₃⁻ and CO₃²⁻ were applied according to Mook et al. (1974) and Zhang et al. (1995),
222 respectively.

223 **Growth**

224 Relative growth rates (RGR) were measured according to Olischläger et al. (2013). The fresh weight
225 was determined to a precision of 1 mg (LA 310S, Sartorius, Göttingen, Germany) after having blotted

226 the thalli carefully between tissue paper until all superficial water was absorbed. RGR was calculated
227 after Lüning (1990):

$$228 \text{ RGR (\% day}^{-1}\text{)} = \frac{100 * \text{Ln}(W1 / W2)}{T1 - T2}$$

229 W1 = Fresh weight (g) in time 1, W2 = Fresh weight (g) in time 2, T1 and T2 = Time in days

230 **Statistics**

231 Two-factorial designs were analyzed with two-way ANOVA ($P < 0.05$) after the homogeneity of
232 variances was confirmed using the Cochran's-test. Post hoc comparisons were performed by Fisher's
233 LSD test ($P < 0.05$). The analyses were performed using Statistica software v.7 (StatSoft Inc, Tulsa,
234 USA). Ecotypic differences were tested at 10°C using a two-factorial ANOVA. The outcome of the
235 statistical analyses testing the effects of elevated pCO₂ and temperature on the SP and the HL
236 population are summarized in Table 1 and 2; the statistical analyses testing the effects of ecotype and
237 pCO₂ at 10°C are summarized in Table 3.

238 **Results**

239 Overall, both populations of *S. latissima* were significantly more affected by temperature than by
240 pCO₂ or the interaction between the two factors (Table 1 and 2), although the responses were different
241 between both populations cultured at 10°C in 70% of those variables (Table 3).

242 **The effects of pCO₂ and temperature on growth and the photosynthetic performance of** 243 **the Helgoland population**

244 The majority of the photosynthetic pigments contents were, on a DW basis, significantly higher at
245 17°C ($P < 0.001$, two-factorial ANOVA; Table 1, Fig. 1 and 2), but only Chl *c*, β-carotene and the
246 xanthophyll cycle pigment pool (VAZ) were significantly altered by pCO₂ ($P < 0.05$, two-factorial
247 ANOVA), showing a general decrease at future pCO₂ conditions, although none of them were
248 influenced by the interaction between both factors. The only one not affected by temperature was
249 antheraxanthin, while zeaxanthin was significantly reduced at 17°C ($P < 0.01$, two-factorial ANOVA),
250 producing a lower DPS of the xanthophyll cycle pigments ($P < 0.001$, two-factorial ANOVA, Fig. 2).

251 When the pigments contents are calculated per Chl *a*, the only significantly temperature-sensitive
252 accessory pigments were fucoxanthin and the xanthophyll cycle pigments ($P < 0.001$, two-factorial
253 ANOVA; Table 2), showing a reduction of zeaxanthin Chl a^{-1} at 17°C ($P < 0.001$, two-factorial
254 ANOVA), and an enhancement of antheraxanthin Chl a^{-1} and violaxanthin Chl a^{-1} at 17°C ($P < 0.01$,
255 two-factorial ANOVA). The latter also showed a significant interaction between temperature and
256 pCO₂ ($P < 0.001$, two-factorial ANOVA). However, the sum of all accessory pigments per Chl *a*,
257 which is an indicator of the antenna size, was not influenced by any of the factors.

258 The $\Delta F/F_m'$ was not significantly affected, either by pCO₂, temperature or the interaction of the two
259 ($P > 0.05$, two-factorial ANOVA; Table 1; Fig. 3). Nevertheless, the photosynthetic O₂ evolution
260 (either referred to DW or to Rubisco content) was significantly higher at the highest tested temperature
261 ($P < 0.001$, two-factorial ANOVA; Fig. 4). However, when the O₂ evolution was referred to the Chl *a*
262 content, there was no significant effect. Elevated pCO₂ did not significantly influence the O₂ evolution
263 referred to DW or Chl *a*, but when the O₂ evolution was referred to Rubisco content, a stimulating
264 influence of elevated pCO₂ was shown, although it was only significant at 17°C ($P < 0.05$, Fisher's
265 LSD test).

266 The content of Rubisco per g of DW and per g of total protein was significantly affected by
267 temperature ($P < 0.01$, two-factorial ANOVA, Table 1; Fig. 5), showing a decrease at higher
268 temperature and current pCO₂ conditions ($P < 0.05$, Fisher's LSD test). Also, elevated pCO₂ produced
269 a decrease in Rubisco content ($P < 0.05$, two-factorial ANOVA), although it was not statistically
270 significant at 17°C ($P > 0.05$, Fisher's LSD test). The content of the D1 protein, a core component of
271 PS II that is involved in PS II damage and repair in photoinhibition, was only significantly altered by
272 pCO₂ ($P < 0.01$, two-factorial ANOVA), showing a decrease at elevated pCO₂ conditions at both
273 temperatures ($P > 0.05$, Fisher's LSD test).

274 The ¹³C isotopic fractionation of organic carbon production (ϵ_p) is primarily controlled by the
275 acquisition and intracellular transport of inorganic carbon and the rate of carbon fixation (Rau et al.
276 1997); thus, it is used as an indicator of the CCMs operation, since the increase in the utilization of
277 isotopically heavier HCO₃⁻ respect to isotopically lighter CO₂ produce a decrease in ϵ_p . Our results

278 showed a significant increase in ϵ_p at higher temperature ($P < 0.001$, two-factorial ANOVA) and
279 increased pCO₂ conditions ($P < 0.001$, two-factorial ANOVA; Table 1, Fig. 6).

280 Neither temperature, nor pCO₂, nor the interaction of both factors significantly influenced the RGR (P
281 > 0.05 , two-factorial ANOVA; Fig. 7).

282 **The effects of pCO₂ and temperature on growth and the photosynthetic performance of** 283 **the Spitsbergen population**

284 Very few significant differences in the photosynthetic pigments contents between treatments were
285 obtained, and most of them were due to temperature but not pCO₂. β -carotene, anthera-, viola-, and
286 zeaxanthin, on a DW basis, were significantly altered by temperature ($P < 0.05$, two-factorial
287 ANOVA; Table 1, Fig. 1 and 2), although the differences were rather small. Thus, DPS was reduced at
288 10°C ($P < 0.001$, two-factorial ANOVA). Zeaxanthin and VAZ were the only ones affected by pCO₂
289 ($P < 0.05$, two-factorial ANOVA), showing a decrease at future pCO₂ conditions, but this decrease
290 was only significant at 10°C ($P < 0.05$; Fisher's LSD test). If the pigment contents are referred to Chl
291 a ; anthera-, viola-, zeaxanthin and VAZ were significantly altered by temperature ($P < 0.05$, two-
292 factorial ANOVA), and Chl c was influenced by the interaction of both factors ($P < 0.05$, two-factorial
293 ANOVA). Nevertheless, the sum of all accessory pigments per Chl a was not altered.

294 Both temperature and pCO₂ ($P < 0.05$, two-factorial ANOVA) affected $\Delta F/F_m'$ significantly, although
295 there was only a significant minor decrease at 4°C combined with future pCO₂ conditions, in
296 comparison with the result obtained at 10°C and present pCO₂ ($P < 0.05$; Fisher's LSD test, Fig. 3).

297 The net photosynthetic rate (referred to DW, Rubisco content or Chl a content) was significantly
298 altered by temperature ($P < 0.05$, two-factorial ANOVA; Fig. 4), showing an increase at 10°C at
299 current pCO₂ conditions ($P < 0.05$; Fisher's LSD test); this difference being stronger when the
300 photosynthetic rate was corrected by Rubisco content. Moreover, the latter was also influenced by the
301 interaction between pCO₂ and temperature ($P < 0.05$, two-factorial ANOVA). Rubisco content
302 (referred to DW or to protein content) was significantly reduced at 10°C ($P < 0.01$, two-factorial
303 ANOVA), although a significant decrease at higher pCO₂, as described above for the HL population,

304 was not found ($P > 0.05$; Fisher's LSD test; Fig. 5). However, D1 content was not altered by
305 temperature, pCO₂ or by the interaction between them.

306 ϵ_p showed a significant influence of pCO₂ ($P < 0.001$, two-factorial ANOVA; Table 1, Fig. 6), with a
307 statistically significant increase at high but not at expected pCO₂ ($P < 0.05$, Fisher's LSD test).

308 Moreover, temperature and pCO₂ significantly affected RGR ($P < 0.05$, two-factorial ANOVA; Fig.
309 7), showing higher values at 10°C, and also at increased pCO₂ compared to current pCO₂ ($P < 0.05$,
310 Fisher's LSD test).

311 **Ecotypic variation and the effects of pCO₂ on growth and the photosynthetic** 312 **performance between the populations**

313 Chl *a* content was significantly higher in the SP population than in the HL population at 10°C,
314 revealing an ecotypic differentiation ($P < 0.001$, two-factorial ANOVA; Table 3, Fig. 1). The content
315 of all accessory pigments were not ecotype-specific, except violaxanthin and antheraxanthin, which
316 showed lower values for the SP population ($P < 0.01$, two-factorial ANOVA; Fig. 2). However, apart
317 from the xanthophyll cycle pigments, the rest of the accessory pigments were altered by pCO₂ ($P <$
318 0.001 , two-factorial ANOVA), following a trend of a decreased content at high pCO₂. Thus, the ratio
319 of the majority of the accessory pigments to Chl *a* was lower in the SP population compared to the HL
320 population, including the sum of all accessory pigments per Chl *a*. However, antheraxanthin Chl *a*⁻¹
321 was higher in the SP population and zeaxanthin Chl *a*⁻¹ showed no response. There was no population-
322 specific difference in the DPS.

323 While there was no ecotypic differentiation for the $\Delta F/F_m'$ ($P > 0.05$, two-factorial ANOVA; Fig. 3),
324 the net photosynthetic rate by O₂ evolution (referred either to DW, Rubisco content or Chl *a* content)
325 was significantly higher in the SP population than in the HL population ($P < 0.001$, two-factorial
326 ANOVA; Fig. 4).

327 Rubisco content per g DW was significantly different between populations ($P < 0.05$, two-factorial
328 ANOVA; Table 3), showing a decrease of Rubisco in the SP population at present pCO₂ compared

329 with the HL population ($P < 0.05$, Fisher's LSD test; Fig. 5), and a significant interaction between
330 ecotype and pCO₂ was also revealed ($P < 0.05$, two-factorial ANOVA). However, the Rubisco content
331 per g of protein was only influenced by pCO₂ ($P < 0.05$, two-factorial ANOVA) and not by ecotype,
332 although it was only significantly reflected in the HL population ($P < 0.05$, Fisher's LSD test). D1
333 content was significantly higher in the SP population ($P < 0.001$, two-factorial ANOVA) and
334 decreased at elevated pCO₂ ($P < 0.05$, two-factorial ANOVA), but again it was only significantly
335 reflected in the HL population ($P < 0.05$, Fisher's LSD test).

336 ϵ_p showed a significant influence of ecotype and pCO₂ ($P < 0.001$, two-factorial ANOVA; Table 3),
337 with lower values for the HL population and increased values for high pCO₂ ($P < 0.05$, Fisher's LSD
338 test; Fig. 6). Moreover, ecotype and pCO₂ affected RGR ($P < 0.05$, two-factorial ANOVA), showing
339 higher values for the HL population in comparison with the SP population, and increased values at
340 expected pCO₂ only for the SP population ($P < 0.05$, Fisher's LSD test; Fig. 7).

341 **Discussion**

342 Our results provide evidences of a different susceptibility of both *S. latissima* populations toward
343 ocean acidification and temperature, indicating ecotypic differentiation, which is reflected in the
344 growth rate response. However, temperature exerted stronger effects in the physiology of both
345 populations than ocean acidification, in agreement with the results obtained by Olischläger et al.
346 (2014) for its biochemical composition.

347 **The effects of temperature and pCO₂ on growth and the photosynthetic performance of** 348 **the Helgoland population of *Saccharina latissima***

349 The unchanged ratios between accessory pigments and Chl *a* suggest that the antenna size of each
350 photosystems (PS) remained constant (Fig. 1), whereas the decrease in Chl *a* content (based on DW) at
351 lower temperatures might indicate a reduction in the quantity of PS. The former is reflected in the
352 temperature insensitivity of the effective quantum yield of the HL population (Fig. 3), showing that
353 the same relative proportion of the incident light was processed at the PS. Consequently, nearly the
354 same amount of light energy per PS was processed, but the total amount of processed energy per g

355 DW was lower. This result could reflect an adaptation to lower temperatures, which led to lower
356 enzymatic reaction rates of carbon acquisition and fixation (Raven and Geider 1988). Therefore, a
357 decrease in the number of PS must be part of the cold-acclimation in the Atlantic *S. latissima*. This
358 conclusion is further supported from the xanthophyll-data, as the total content of xanthophylls (based
359 on DW) decreased at low temperatures in the HL population (Fig. 2), whereas the content of
360 xanthophylls per Chl *a* only changed at high pCO₂, indicating an interaction between both factors.
361 However, the higher antheraxanthin content and the unchanged zeaxanthin content (based on DW) at
362 10°C, which produced an enhancement of DPS values, suggest that, per PS, more light was dissipated
363 as heat at low temperatures.

364 The lower pigment contents and the evidence for a lower amount of PS II measured at 10°C explain
365 the reduced rate of O₂ production per DW (Fig. 4). Moreover, there was no temperature-dependent
366 difference if the O₂ production rate is referred to Chl *a*, supporting the above conclusion that the
367 produced O₂ per PS II was equal at both temperatures but there was a lower amount of PS.
368 Nevertheless, the temperature sensitivity is revealed if we calculate the amount of O₂ per unit of
369 Rubisco. Assuming that one molecule of O₂ is equivalent to one fixed CO₂ (Al-Najar et al. 2012), the
370 reason for the lower O₂ production rate referred to Rubisco content was the decreased activity of the
371 enzyme at low temperatures (Raven and Geider 1988), which could be partially compensated by the
372 higher Rubisco content observed at 10°C (based on DW or protein content, Fig. 5). Further factors in
373 algae decreasing the amount of produced O₂ could be the oxygenase reaction of Rubisco (the so called
374 photorespiration) and the pseudocyclic electron transport (also called water-water cycle) (Sültemeyer
375 et al. 1993; Leboulanger et al. 1998). According to Olischläger and Wiencke (2013), photorespiration
376 at low temperatures can occur when the carbon acquisition mechanisms are operating at its limits and
377 the alga is unable to further enhance its CCM capacity. A shortage in the CO₂ supply would also
378 hamper the electron drain from the photosynthetic electron transport chain and favor the O₂ fixation
379 via pseudocyclic electron transport, unavoidably leading to an increased formation of reactive oxygen
380 species (ROS; Sültemeyer et al. 1993). However, the ¹³C isotopic fractionation of organic carbon
381 production (ϵ_p) for the HL population decreased at 10°C (Fig. 6). This result suggests a preference for
382 bicarbonate use as inorganic carbon source, which is enriched in ¹³C compared to CO₂, leading to a

383 higher fixation of ^{13}C by Rubisco. Thus, the decreased ϵ_p indicated an increased activation of CCMs at
384 10°C , which could partially compensate the decreased catalytic activity of Rubisco. This enhanced
385 activation might be fuelled by an increased cyclic electron flow around PS I (Giordano et al. 2005),
386 which is thought to act as a photoprotection mechanism at low temperatures (Clarke and Johnson
387 2001). Moreover, the suspected reduced number of PS at 10°C was not significantly reflected in a
388 reduced D1 content (Fig. 5). The content of D1 protein must be the result of a balance between
389 damage of the D1 protein and replacement of the damaged protein by a newly synthesized D1
390 polypeptide, which have an energetic cost (Raven 2011). Thus, our results might indicate a higher
391 turnover of the protein at 10°C , which can be related to an increased investment in photoprotection
392 mechanisms at low temperatures, as mentioned above.

393 Despite the higher photosynthetic rates indicated by O_2 evolution measurements at 17°C , the growth
394 rates were unaltered by temperature (Fig. 7). This could suggest a change of the photosynthetic
395 quotient (PQ) between both temperatures due to different metabolic requirements, indicating a higher
396 investment of photosynthetic energy into processes other than carbon fixation at higher temperatures
397 (Iñiguez et al. 2015). Another explanation for the differences between photosynthetic O_2 evolution and
398 growth rate could be an increase of carbon accumulation and excretion at 17°C . Our data show that, in
399 contrast to slightly lower contents of carbohydrates, lipids and proteins (Olischläger et al. 2014), the
400 content of soluble phlorotannins (Fig. S1) was higher at elevated temperature, indicating that
401 secondary metabolites, such as phlorotannins, may be the final sink of the additionally fixed C which
402 was not invested into growth. This could be related also to an increase in the release of dissolved
403 organic carbon (DOC) at higher temperatures, which has been also observed in other species
404 (Borchard and Engel 2012; Iñiguez et al. 2015).

405 The impact of elevated pCO_2 on the physiology of the HL population is lower than the impact of
406 increased temperature. The only pigment contents affected by elevated pCO_2 were Chl *c*, VAZ and β -
407 carotene, although there were no change in these pigment contents corrected by Chl *a* (Fig. 1 and 2).

408 The lower β -carotene content at elevated pCO_2 could occur in response to a decreased need to detoxify
409 ROS. ROS production might be favored at low pCO_2 (Vardi et al. 1999; García-Gómez et al. 2014) in

410 response to a CO₂-shortage, and algal β-carotene might participate in the antioxidant mechanisms
411 (Holdt and Kraan 2011). A shortage of CO₂ can result in a shortage of NADP⁺, the final oxidant of the
412 photosynthetic electron transport chain, which in turn would increase the excitation state of the
413 photosynthetic electron transport chain and would favour the production of ROS (Sitte et al. 2002).
414 Thus, the higher β-carotene content at present pCO₂ compared to high pCO₂ might prevent cells from
415 photoinhibition, the latter being reflected in a higher degradation of the D1 protein by increased
416 production of ROS (Lesser 2006, Fig. 5) and, consequently, in a lower effective quantum yield; a
417 response which was not observed in our data.

418 At 10°C, Chl *a* content decreased at high pCO₂ without a change in the ratio accessory pigments Chl *a*⁻¹
419 ¹, indicating a lower content of PS, which suggest a decrease in photosynthetic energy demand due
420 presumably to deactivation of CCMs, as shown by ε_p data (Fig. 6). This results are in agreement with
421 the reduction observed in the D1 content at high pCO₂. Furthermore, at 17°C, the energy saved by
422 deactivation of CCMs at increased pCO₂ might have been invested in an increased accumulation of
423 carbohydrates (Olischläger et al. 2014), as the unchanged content of Chl *a* and the ratio accessory
424 pigment Chl *a*⁻¹ suggest that the content of PS was not altered. However, the decrease in the D1
425 content observed at 17°C and elevated pCO₂ might reflect a higher rate of degradation or a slower rate
426 of reposition than at present pCO₂.

427 Elevated pCO₂ decreased the amount of Rubisco per DW and per protein content, although at 17°C,
428 this reduction was not statistically significant (Fig. 5). Since elevated pCO₂ does not change the O₂
429 production rate on a DW basis, the significantly higher photosynthetic O₂ production per mg of
430 Rubisco obtained could reflect that, at present pCO₂, Rubisco was not C-saturated despite CCM
431 functioning. Thus, a lower quantity of this enzyme was able to maintain the same photosynthetic rate
432 at high pCO₂. Lower protein content at increased CO₂ has been observed earlier in the chlorophyte
433 seaweed *Ulva rigida* (Gordillo et al. 2001). Other studies have shown that CCMs in Laminariales are
434 weak compared to other intertidal brown algae (Surif and Raven 1989; Haglund et al. 1992), and it
435 might be possible that CCM function increases Rubisco activity but does not completely saturate the
436 enzyme.

437 All this physiological pCO₂ and temperature driven re-arrangement led to an unchanged RGR, which
438 was apparently at its maximum and potentially limited by the meristematic capacity, as it was neither
439 temperature nor pCO₂-sensitive (Fig. 7, see Koch et al. 2013; Harley et al. 2012; Gao et al. 2012)

440 **The effects of pCO₂ and temperature on growth and the photosynthetic performance of** 441 **the Spitsbergen population of *Saccharina latissima***

442 According to the Chl *a* and accessory pigments content, comparable amounts of photons were
443 harvested at both temperatures tested. Only β-carotene and the xanthophyll cycle pigments
444 individually, were significantly affected by temperature with a rather small effect (Fig. 1). Hence,
445 neither the number of PS nor the photosystem-antenna size was strongly affected in the tested
446 temperature range. Consequently, comparable amounts of accessory pigments might have transported
447 similar amounts of photons towards the reaction centers of the PS at both temperatures (Fig. 1, Fig. 2),
448 despite an enhanced energy dissipation due to an increased anthera- and zeaxanthin content at lower
449 temperature, which is translated in a higher DPS.

450 The small but significant decrease of the effective quantum yield at low temperature in the SP
451 population could indicate a higher non-photochemical dissipation of energy in PS II (Fig. 3), as shown
452 by the significantly higher value of DPS (Fig. 2). However, the temperature effect on light harvesting
453 and effective quantum yield cannot explain the proportion of decrease in O₂ production rate at 4°C
454 (irrespective of it being expressed on the basis of DW, Chl *a*, or Rubisco content). This might be a
455 consequence of increased photorespiration, an enhancement of the water-water cycle and/or an
456 activation of cyclic electron flow around PS II, as all these processes may alter net O₂ production rate
457 without affecting the effective quantum yield of PS II. Cyclic electron flow around PS II could act as
458 part of a photoprotection strategy, dissipating excess of excitation energy even at subsaturating
459 irradiances at low temperatures, when the metabolic activity is reduced such that its capacity is
460 exceeded by the absorption of light by the photosynthetic apparatus. This mechanism was also
461 suggested for *U. rigida* by Gordillo et al. (2003) and for the diatom *Phaeodactylum tricornutum* by
462 Feikema et al. (2006). Moreover, the water-water cycle and the cyclic electron flow around PS I have
463 also been proposed as photoprotection mechanisms for the consumption of photons under conditions

464 where the rate of photosynthetic electron transport exceeds the capacity of the C metabolism, leading
465 to increased thylakoid acidification required for the de-epoxidation of violaxanthin to zeaxanthin and
466 the non-photochemical dissipation of excess excitation energy (Horton et al. 1996). However, unlike
467 the Mehler reaction, cyclic electron flow around PS I does not have the associated problem of harmful
468 free-radical production, as the enzymes for detoxification of radicals would be slowed down at low
469 temperature (Clarke and Johnson 2001). Thus, an increase in the photoprotection mechanisms at low
470 temperatures would help to dissipate excess of photons and, unavoidably, decrease the carbon fixation
471 (and growth rate) by producing an excess of ATP over that needed in CO₂ assimilation. This increased
472 ATP production might support the maintenance of a similar CCM activity at low temperature (Fig. 6).
473 Furthermore, an enhanced production of intra-chloroplastic ROS, as a consequence of photoinhibition
474 at low temperatures, is not supported by a higher content of antioxidants, such as β-carotene and
475 phlorotannins (see Fig. 1S), or by a change in the D1 protein content. An additional reason for the
476 decreased growth rate at 4°C could be a higher accumulation of lipids, as shown in Olischläger et al.
477 (2014), serving as an energetic reserve for growth during the polar night (Bartsch et al. 2008).

478 As has been shown for HL population, the impact of pCO₂ on the physiology of the SP population was
479 also lower than the impact of temperature. The effective quantum yield at 4°C was slightly lower at
480 elevated pCO₂, which could suggest a photochemical stress, a higher heat dissipation or a reduced
481 light harvesting. However, the assumption of a photochemical stress is not supported by the CO₂-
482 insensitive O₂ evolution, the CO₂-stimulated growth or the unchanged D1 content. Moreover, a higher
483 heat dissipation is not supported either by the decrease in the zeaxanthin content at high CO₂ or the
484 unchanged DPS values, and there was no significant effect in the amount of PS or the PS antenna
485 size that could further point to an increased light harvesting. Despite the unchanged net photosynthetic
486 rate, the increased growth at elevated pCO₂ could suggest a reduced loss of carbon, mainly by
487 decreasing respiration and/or DOC excretion, as proposed by Gordillo et al. (2001) for *U. rigida* and
488 Iñiguez et al. (2015) for the Arctic kelp *Alaria esculenta*. This indicates that the cell division rate of
489 the meristem is apparently not maximal. According to Körner (2012), under those conditions the
490 meristematic growth could be stimulated by the provision of additional resources. This response has
491 been previously reported at elevated pCO₂ (de Castro Araújo and Tarvano García 2005; Olischläger

492 and Wiencke 2013; Sarker et al. 2013). The reason why high pCO₂ (1500 μatm pCO₂) did not
493 stimulate growth at 10°C remains unclear, but it is a frequent phenomenon reported in previous studies
494 (Kübler et al. 1999; Diaz-Pulido et al. 2011). An hypothesis for that fact could be a different
495 sensitivity to changes in external pH between the studied temperatures, leading to a higher DOC
496 excretion and/or a reallocation of the energy saved due to CCM deactivation (as suggested by ε_p data,
497 see Fig. 6). Potentially, the difference in growth between 800 μatm and 1500 μatm pCO₂ can be linked
498 to a stimulated Rubisco content at 10°C and 800 μatm pCO₂, which was not observed at high pCO₂
499 (Fig. 5). In contrast to the HL population, Rubisco content of the Arctic ecotype was not decreased at
500 high pCO₂, and the net photosynthetic rate per mg of Rubisco was not altered, indicating that Rubisco
501 was already CO₂-saturated at present CO₂ concentrations.

502 **Ecotypic variation and the effect of pCO₂ on both populations**

503 When the physiology of the SP and the HL populations are compared under equal conditions (10°C),
504 pronounced differences between their physiological performance could be observed. The Chl *a*
505 content of the SP population was higher (Fig. 1), whereas the total content of accessory pigments was
506 not different, giving a lower ratio of accessory pigments Chl *a*⁻¹. Thus, the number of PS of the Arctic
507 population should be higher and the antenna size smaller than in the cold-temperate population (Fig.
508 1), which might reflect an adaptation that avoids photoinhibition in cold environments. Hence, the
509 excitation pressure on the PS was lower in the SP population, a finding which might be reflected in the
510 lower investment in protective means against excessive excitation, such as the xanthophyll cycle (Fig.
511 2). Remarkable is that, despite the lower antenna size and xanthophyll content and the reduced
512 investment in active carbon acquisition, the O₂ evolution was clearly higher in the SP population, in
513 parallel to a lower content of Rubisco per g DW. The latter suggests that, at 10°C, the carbon fixation
514 rate was more efficient in the SP population, suggesting changed kinetic characteristics between
515 Rubisco of the two populations (Morgan-Kiss et al. 2006). Conclusively, the physiological data reveal
516 that the photosynthetic performance of SP population at 10°C is better than that of the HL population,
517 clearly indicating shifted temperature sensitivity between both populations and revealing ecotypic
518 differentiation. However, this improved physiological performance was not reflected in higher growth

519 rates for SP population; contrastingly, the growth of the HL population was even higher at 10°C. This
520 might be a consequence of higher contents of storage metabolites, such as lipids and carbohydrates in
521 the SP population, as it has been shown in Olischläger et al. (2014). As previously reported, the Arctic
522 population is adapted to store a higher fraction of the produced photosynthates during nutrient-
523 depleted summer, likely serving as energy reserve for the nutrient-repleted long polar night, when
524 most of the growth takes place (Bartsch et al. 2008).

525 pCO₂ drove some similar responses in both ecotypes. Most of the pigments contents per DW analysed
526 tend to decrease at elevated pCO₂, even though Chl *a* and accessory pigments Chl *a*⁻¹ were not
527 significantly affected, and also ε_p values suggest that CCMs seemed to be at least partially deactivated
528 at high CO₂ in both ecotypes. However, deactivation in both populations at 10°C occurred only at high
529 CO₂ concentrations (1500 μatm) but it was not appreciated at 800 μatm, although the HL population
530 already showed a deactivation at 800 μatm CO₂ at 17°C. This could indicate a higher need of CCM
531 activity at low temperatures, as suggested before by Gordillo et al. (2016).

532 There were very few significant interactions between ecotypes and pCO₂. In the HL population,
533 expected and future pCO₂ levels decreased the content of Rubisco per DW, whereas in the SP
534 population, the content of Rubisco increased at predicted pCO₂, but not at high pCO₂. It is known that
535 the algal response to elevated pCO₂ is dependent on the applied pCO₂, and bell-shaped responses in
536 growth rates were previously reported (Kübler et al. 1999; Diaz-Pulido et al. 2011). This is
537 remarkable, since the presented bell-shaped pattern for the Rubisco content in the SP population at
538 10°C was mirrored by the growth pattern, whereas the growth-pattern of the HL-population
539 (insensitive to elevated pCO₂) did not reflect the significantly lower Rubisco content. This is
540 potentially attributable to the degree of activation of the enzyme Rubisco, since in polar algae,
541 Rubisco appears to be almost completely activated and at near CO₂ saturation, achieving the high
542 carbon fixation rates observed (Young et al. 2015), whereas the temperate population could have a
543 higher degree of Rubisco deactivation in some circumstances. Also, this fact could be related to the
544 previously discussed ecotype-specific differences in the degree of utilization of the meristems at 10°C

545 and/or an ecotypic difference in the allocation of the photosynthates towards storage metabolites or
546 growth (Bartsch et al. 2008; Olischläger et al. 2014).

547 **Conclusion**

548 The Arctic and the cold-temperate populations of *S. latissima* represent different ecotypes with
549 striking differences in their physiology. Both populations were sensitive to changing temperatures and
550 OA, but to different extent. Changes in temperature seems to exert a stronger effect than pCO₂ in the
551 physiology of both populations. Concerning growth, the Arctic-ecotype was more sensitive to pCO₂,
552 particularly at low, apparently suboptimal temperatures, compared to the Atlantic ecotype; although
553 the biochemical composition of the Arctic-ecotype was more CO₂-insensitive, as shown by
554 Olischläger et al. (2014) and data from pigment, D1 and Rubisco content shown in the present study.
555 This fact reflects different acclimation strategies for both populations. The growth rate response of the
556 Arctic population at increased temperature is most likely attributable to an incomplete adaptation to
557 the cold environment, which *S. latissima* reinvaded after the last deglaciation event approximately
558 18000 years ago (Lüning 1990). Our findings show that the Arctic ecotype might benefit from global
559 warming and, in a lesser extent, ocean acidification, with potentially large consequences for the
560 current Arctic phytobenthic community and the associated fauna, as it has been suggested by other
561 studies (Gordillo et al. 2015); while *S. latissima* from temperate latitudes, with an unaltered growth
562 rate, is suspected not to be strongly affected by ocean acidification and increased temperature.

563 **Author contribution**

564 MO, CI planned the experiments; MO and CI conducted the experiments and did the required
565 measurements. MO and CI did the statistical analysis of the data and wrote most parts of the
566 manuscript with the assistance and the discussion of all coauthors. All authors contributed to the
567 writing process and all authors read and approved the manuscript.

568 **Acknowledgments**

569 This is a CEI-MAR publication, partly financed by project CTM2011-24007 from the Spanish
570 Ministry of Science and Innovation. This work was also partly funded by the German Federal Ministry
571 for Science and Education (BMBF; Förderkennzeichen 03F0608B) as part of the BIOACID program
572 (subproject 4.1.1). Furthermore, we wish to thank Andreas Wagner and Claudia Daniel for assistance
573 with lab work.

574 **References**

575 Al-Najjar MAA, de Beer D, Kühl M, Polerecky L (2012) Light utilization efficiency in photosynthetic
576 microbial mats. *Environ Microbiol* 14:982–992

577 Andría JR, Brun FG, Pérez-Llorens JL, Vergara JJ (2001) Acclimation responses of *Gracilaria* sp.
578 (Rhodophyta) and *Enteromorpha intestinalis* (Chlorophyta) to changes in the external inorganic
579 carbon concentration. *Bot Mar* 44:361–370

580 Bartsch I, Wiencke C, Bischof K, Buchholz CM, Buck BH, Eggert A, Feuerpfeil P, Hanelt D,
581 Jacobsen S, Karez R, Karsten U, Molis, M, Roleda MY, Schubert H, Schumann R, Valentin K,
582 Weinberger F, Wiese J (2008) The genus *Laminaria* sensu lato: recent insights and developments. *Eur*
583 *J Phycol* 43:1–86

584 Borchard C, Engel A (2012) Organic matter exudation by *Emiliania huxleyi* under simulated future
585 ocean conditions. *Biogeosciences* 9:3405–3423

586 Clarke JE, Johnson GN (2001) *In vivo* temperature dependence of cyclic and pseudocyclic electron
587 transport in barley. *Planta* 212:808–816

588 Colombo-Pallotta MF, García-Mendoza E, Ladah LB (2006) Photosynthetic performance, light
589 absorption, and pigment composition of *Macrocystis pyrifera* (Laminariales, Phaeophyceae) blades
590 from different depths. *J Phycol* 42:1225–1234

591 de Castro Araújo S, Tavano Garcia VM (2005) Growth and biochemical composition of the diatom
592 *Chaetoceros* cf. *wighamii* bright well under different temperature, salinity and carbon dioxide levels. I.
593 Protein, carbohydrates and lipids. *Aquaculture* 246:405–412

594 Diaz-Pulido G, Gouezo M, Tilbrook B, Dove S, Anthony K (2011) High CO₂ enhances the
595 competitive strength of seaweeds over corals. *Ecol Lett* 14:156–162

596 Dickson AG (1990) Standard potential of the reaction—AgCl(s) + 1/ 2H₂(G) =AG(g) + HCl(aq) and
597 the standard acidity constant of the ion HSO₄⁻ in synthetic sea-water from 273.15 K to 318.15K. *J*
598 *Chem Thermodyn* 22:113–127

599 Feikema WO, Marosvölgyi MA, Lavaud J, van Gorkom HJ (2006) Cyclic electron transfer in
600 photosystem II in the marine diatom *Phaeodactylum tricornutum*. *Biochim Biophys Acta* 1757:829–
601 834

602 Feng Y, Warner ME, Zhang Y, Sun J, Fu FX, Rose JM, Hutchins DA (2008) Interactive effects of
603 increased pCO₂, temperature and irradiance on the marine coccolithophore *Emiliana huxleyi*
604 (Prymnesiophyceae). *Eur J Phycol* 43:87–98

605 Freeman HJ, Hayes JM (1992) Fractionation of carbon isotopes by phytoplankton and estimates of
606 ancient CO₂ levels. *Global Biogeochem Cycles* 6:185–198

607 Fu FX, Warner ME, Zhang YH, Feng YY, Hutchins DA (2007) Effects of increased temperature and
608 CO₂ on photosynthesis, growth, and elemental ratios in marine *Synechococcus* and *Prochlorococcus*
609 (Cyanobacteria). *J Phycol* 43:485–496

610 Gao K, Xu J, Gao G, Li Y et al (2012) Rising CO₂ and increased light exposure synergistically reduce marine
611 primary productivity. *Nat Clim Change* 2: 519–523

612 García-Gómez C, Gordillo FJL Palma A, Lorenzo RM, Segovia M (2014) Elevated CO₂ alleviates
613 high PAR and UV stress in the unicellular chlorophyte *Dunaliella tertiolecta*. *Photochem Photobio Sci*
614 13:1347–1358

615 García-Sánchez MJ, Fernández JA, Niell X (1994) Effect of inorganic carbon supply on the
616 photosynthetic physiology of *Gracilaria tenuistipitata*. *Planta* 194:55–61

617 Giordano M, Beardall J, Raven JA (2005) CO₂ concentrating mechanisms in algae: mechanisms,
618 environmental modulation and evolution. *Annu Rev Plant Biol* 56:99–131 Gordillo FJL, Aguilera J,

619 Jimenez C (2006) The response of nutrient assimilation and biochemical composition of Arctic
620 seaweeds to a nutrient input in summer. *J Exp Bot* 57:2661–2671

621 Gordillo FJL, Aguilera J, Wiencke C, Jiménez C (2015) Ocean acidification modulates the response of
622 two Arctic kelps to ultraviolet radiation. *J Plant Physiol* 173:41–50

623 Gordillo FJL, Carmona R, Viñegla B, Wiencke C, Jiménez C (2016) Effects of simultaneous increase
624 in temperature and ocean acidification on biochemical composition and photosynthetic performance of
625 common macroalgae from Kongsfjorden (Svalbard). *Polar Biol* DOI 10.1007/s00300-016-1897-y

626 Gordillo FJL, Figueroa FL, Niell FX (2003) Photon- and carbon-use efficiency in *Ulva rigida* at
627 different CO₂ and N levels. *Planta* 218:315–322

628 Gordillo FJL, Jiménez C, Figueroa FL, Niell FX (1999) Effects of increased atmospheric CO₂ and N
629 supply on photosynthesis, growth and cell composition of the cyanobacterium *Spirulina platensis*
630 (*Arthrospira*). *J Appl Phycol* 10:461–469

631 Gordillo FJL, Niell FX, Figueroa FL (2001) Non-photosynthetic enhancement of growth by high CO₂
632 level in the nitrophilic seaweed *Ulva rigida* C. Agardh (Chlorophyta). *Planta* 213:64–70

633 Haglund K, Ramazanov Z, Mtolera M and Pedersen M (1992) Role of external carbonic anhydrase in
634 light-dependent alkalization by *Fucus serratus* L. and *Laminaria saccharina* (L.) Lamour.
635 (Phaeophyta). *Planta* 188:1–6

636 Harley CDG, Anderson KM, Demes KW, Jorve JP, Kordas RL, Coyle TA (2012) Effects of climate
637 change on global seaweed communities. *J Phycol* 48:1064–1078

638 Hepburn CD, Pritchard DW, Cornwall CE, McLeod RJ, Beardall, J, Raven JA, Hurd CL (2011)
639 Diversity of carbon use strategies in a kelp forest community: implications for a high CO₂ ocean. *Glob*
640 *Change Biol* 17:2488–2497

641 Holdt SL, Kraan S (2011) Bioactive compounds in seaweed: functional food applications and
642 legislation. *J Appl Phycol* 23:543–597

643 Horton P, Ruban AV, Walters RG (1996) Regulation of light harvesting in green plants. *Annu Rev*
644 *Plant Physiol Plant Mol Biol* 47:655–684

645 Iñiguez C, Carmona R, Lorenzo MR, Niell FX, Wiencke C, Gordillo FJL (2015) Increased CO₂
646 modifies the carbon balance and the photosynthetic yield of two common Arctic brown seaweeds:
647 *Desmarestia aculeata* and *Alaria esculenta*. *Polar Biol* DOI: 10.1007/s00300-015-1724-x

648 Koch M, Bowes G, Ross C, Zhang XH (2013) Climate change and ocean acidification effects on
649 seagrasses and marine macroalgae. *Glob Change Biol* 19:103–132

650 Körner C (2012) Angebot oder Nachfrage: Was steuert das Pflanzenwachstum. *Biologie in unserer*
651 *Zeit* 42:228–243

652 Kübler JE, Johnston AM, Raven JA (1999) The effects of reduced and elevated CO₂ and O₂ on the
653 seaweed *Lomentaria articulata*. *Plant Cell Environ* 22:1303–1310

654 Laemmli UK (1970) Cleavage of structural proteins during the assembly of the head of bacteriophage
655 T4. *Nature* 227:680–685

656 Leboulanger C, Martin-Jézéquel V, Descolas-Gros C, Sciandra A, Jupin HJ (1998) Photorespiration in
657 continuous culture of *Dunaliella tertiolecta* (Chlorophyta): Relationships between Serine, Glycine and
658 extracellular glycolate. *J Phycol* 34:651–654

659 Lesser MP (2006) Oxidative stress in marine environments: Biochemistry and physiological ecology.
660 *Annu Rev Physiol* 68:253–278

661 Lüning K (1990) Seaweeds. Their environment biogeography and ecophysiology. Wiley-Interscience
662 Publication, New York

663 Maxwell K, Johnson GN (2000) Chlorophyll fluorescence - a practical guide. *J Exp Bot* 51:659–668

664 Millero FJ, Graham TB, Huang F, Bustos-Serrano H, Pierrot D (2006) Dissociation constants of
665 carbonic acid in seawater as a function of salinity and temperature. *Mar Chem* 100:80–94

666 Mook WG, Bommerso JC, Staverma WH (1974) Carbon isotope fractionation between dissolved
667 bicarbonate and gaseous carbon-dioxide. *Earth Planet Sci Lett* 22:169–176

668 Morgan-Kiss RM, Prisco JC, Poccock T, Gudynaite-Savitch L, Huner NPA (2006) Adaptation and
669 acclimation of photosynthetic microorganisms to permanently cold environments. *Microbiol Mol Biol*
670 *R* 70:222–252

671 Müller R, Wiencke C, Bischof K (2008) Interactive effects of UV radiation and temperature on
672 microstages of Laminariales (Phaeophyceae) from the Arctic and North Sea. *Clim Res* 37:203–213

673 Neuhoff V, Arnold N, Taube D, Ehrhardt W (1988) Improved staining of proteins in polyacrylamide
674 gels including isoelectric focusing gels with clear background at nanogram sensitivity using
675 Coomassie Brilliant Blue G-250 and R-250. *Electrophoresis* 9:255–262

676 Olischläger M, Bartsch I, Gutow L, Wiencke C (2012) Effects of ocean acidification on different life-
677 cycle stages of the kelp *Laminaria hyperborea* (Phaeophyceae). *Bot Mar* 55:511–525

678 Olischläger M, Bartsch I, Gutow L, Wiencke C (2013) Effects of ocean acidification on growth and
679 physiology of *Ulva lactuca* (Chlorophyta) in a rockpool-scenario. *Phycol Res* 61:180–190

680 Olischläger M, Iñiguez C, Gordillo FJL, Wiencke C (2014) Biochemical composition of temperate and
681 Arctic populations of *Saccharina latissima* after exposure to increased pCO₂ and temperature reveals
682 ecotypic variation. *Planta* 240:1213–1224

683 Olischläger M, Wiencke C (2013) Ocean acidification alleviates low temperature effects on growth
684 and photosynthesis of the red alga *Neosiphonia harveyi* (Rhodophyta). *J Exp Bot* 64:5587–5597

685 Pfündel E, Bilger W (1994) Regulation and possible function of the violaxanthin cycle. *Photosynth*
686 *Res* 42:89–109

687 Provasoli L (1968) Media and prospects for the cultivation of marine algae. Japanese Society for Plant
688 Physiology, Tokyo, Cultures and collections of algae. In: Proceedings of the US–Japan conference,
689 Hakone 1966, pp 63–75

690 Rau GH, Riebesell U, Wolf-Gladrow D (1997) CO_{2aq}-dependent photosynthetic ¹³C fractionation in
691 the ocean: A model versus measurements. *Global Biogeochem Cycles* 11(2):267–278

692 Raven JA (2011) The cost of photoinhibition. *Physiol Plant* 142:87–104

693 Raven JA, Beardall J (2003) Carbon acquisition mechanisms of algae: carbon dioxide diffusion and
694 carbon dioxide concentrating mechanisms. In: Larkum AW, Douglas SE, Raven JA (eds)
695 Photosynthesis in algae. *Advances in photosynthesis and respiration*. Vol. Kluwer Academic
696 Publishers, The Netherlands, pp 225–244

697 Raven JA, Beardall J (2016) The ins and outs of CO₂. *J Exp Bot* 67(1):1–13

698 Raven JA, Geider RJ (1988) Temperature and algal growth. *New Phytol* 110:441–461

699 Raven JA, Giordano M, Beardall J, Maberly SC (2012) Algal evolution in relation to atmospheric
700 CO₂: carboxylases, carbonconcentrating mechanisms and carbon oxidation cycles. *Phil Trans R Soc B*
701 367:493–507

702 Raven JA, Johnston AM, Kubler JE, Korb R, McInroy SG, Handley LL, Scrimgeour CM, Walker DI,
703 Beardall J, Clayton MN, Vanderklift M, Fredriksen S, Dunton KH (2002) Seaweeds in cold seas:
704 evolution and carbon acquisition. *Ann Bot London* 90:525–536

705 Riebesell U, Fabry VJ, Hansson L, Gattuso JP (2010) *Guide to Best Practices for Ocean Acidification*
706 *Research and Data Reporting*. Luxembourg: Publications Office of the European Union

707 Rokitta SD, Rost B (2012) Effects of CO₂ and their modulation by light in the life-cycle stages of the
708 coccolithophore *Emiliana huxleyi*. *Limnol Oceanogr* 57:607–618

709 Sarker MY, Bartsch I, Olischläger M, Gutow L, Wiencke C (2013) Combined effects of CO₂,
710 temperature, irradiance and time on the physiological performance of *Chondrus crispus* (Rhodophyta).
711 *Bot Mar* 56:63–74

712 Segovia M, Mata T, Palma A, García-Gómez C, Lorenzo R, Rivera A, Figueroa FL (2015) *Dunaliella*
713 *tertiolecta* (Chlorophyta) avoids cell death under ultraviolet radiation by triggering alternative
714 photoprotective mechanisms. *Photochem Photobiol* 91:1389–1402

715 Sitte P, Weiler EW, Kadereit JW, Bresinsky A, Körner C (2002) Strasburger; Lehrbuch der Botanik,
716 Spektrum Akademischer Verlag, Heidelberg Berlin

717 Sültemeyer D, Biehler K, Fock HP (1993) Evidence for the contribution of pseudocyclic
718 photophosphorylation to the energy requirement of the mechanism for concentrating inorganic carbon
719 in *Chlamydomonas*. *Planta* 189:235–242

720 Surif MB, Raven JA (1989) Exogenous inorganic carbon-sources for photosynthesis in seawater by
721 members of the Fucales and the Laminariales (Phaeophyta) – ecological and taxonomic implications.
722 *Oecologia* 78:97–105

723 Takahashi T, Williams RT, Bos DL (1982) Carbonate chemistry. In: Broecker WS, Spencer DW,
724 Craig H (eds) GEOSECS Pacific expedition, vol. 3, Hydrographic Data 1973–1974. National Science
725 Foundation, Washington, pp 77–83

726 Vardi A, Berman-Frank I, Rozenberg T, Hadas O, Kaplan A, Levine A (1999) Programmed cell death
727 of the dinoflagellate *Peridinium gatunense* is mediated by CO₂ limitation and oxidative stress. *Curr*
728 *Biol* 9:1061–1064

729 Wiencke C, Fischer G (1990) Growth and stable carbon isotope composition of cold-water macroalgae
730 in relation to light and temperature. *Mar Ecol Prog Ser* 65:283–292

731 Wright SW, Jeffrey SW, Mantoura RFC, Llewellyn CA, Bjørnland T, Repeta D, Welschmeyer N
732 (1991) Improved HPLC method for the analysis of chlorophylls and carotenoids from marine
733 phytoplankton. *Mar Ecol Prog Ser* 77:183–96

734 Xu Z, Zou D, Gao K (2010) Effects of elevated CO₂ and phosphorus supply on growth, photosynthesis
735 and nutrient uptake in the marine macroalga *Gracilaria lemaneiformis* (Rhodophyta). *Bot Mar*
736 53:123–129

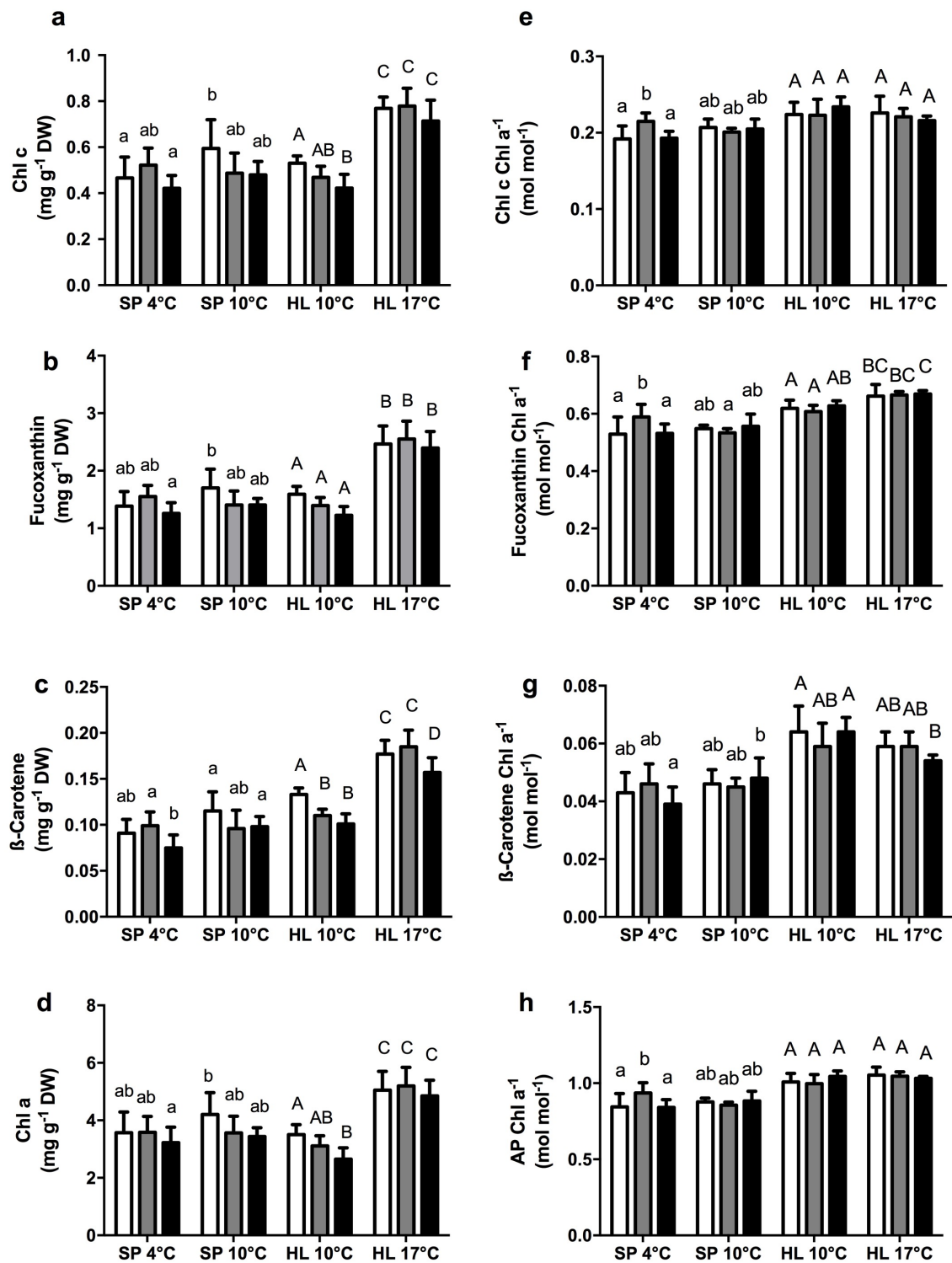
737 Young JN, Goldman JAL, Kranz SA, Tortell PD, Morel FMM (2015) Slow carboxylation of Rubisco
738 constrains the rate of carbon fixation during Antarctic phytoplankton blooms. *New Phytol* 205:172–
739 181

740 Zeebe R, Wolf-Gladrow DA (2001) *CO₂ in Seawater: Equilibrium, Kinetics, Isotopes*. Amsterdam,
741 The Netherlands: Elsevier Science

742 Zhang J, Quay PD, Wilbur DO (1995) Carbon isotope fractionation during gas-water exchange and
743 dissolution of CO₂. *Geochim Cosmochim Acta* 59:107–114

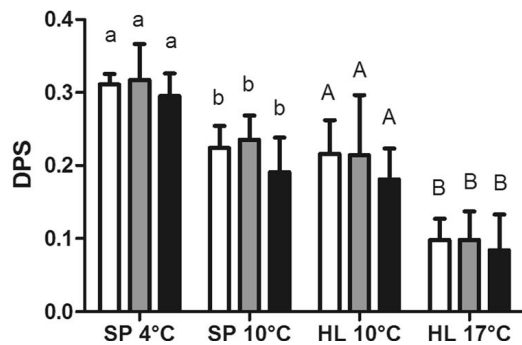
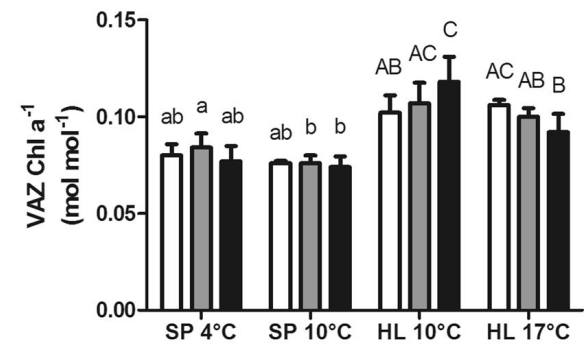
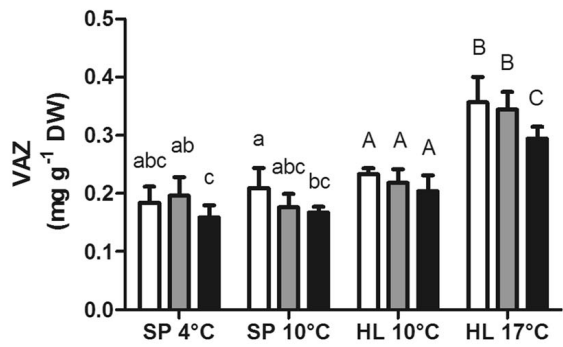
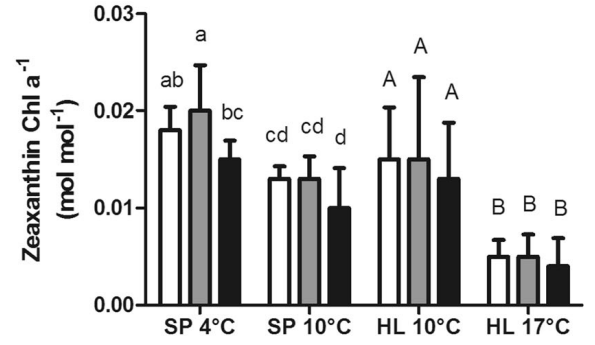
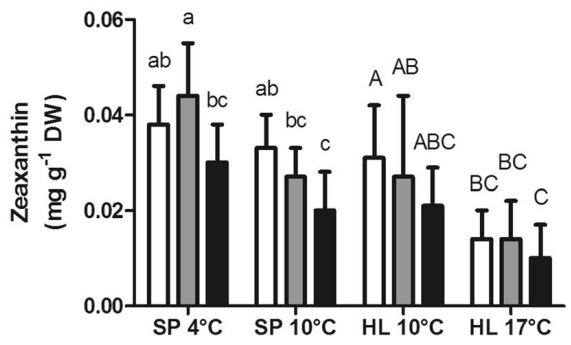
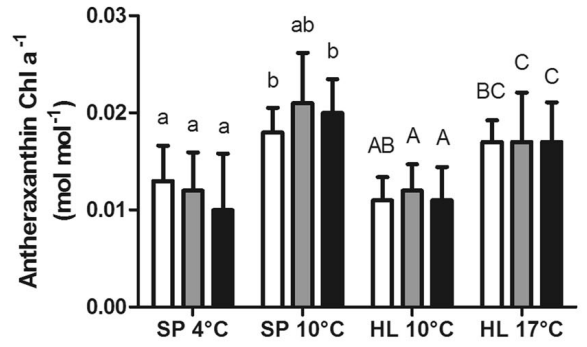
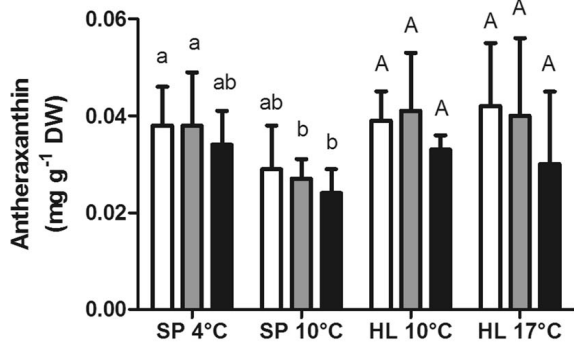
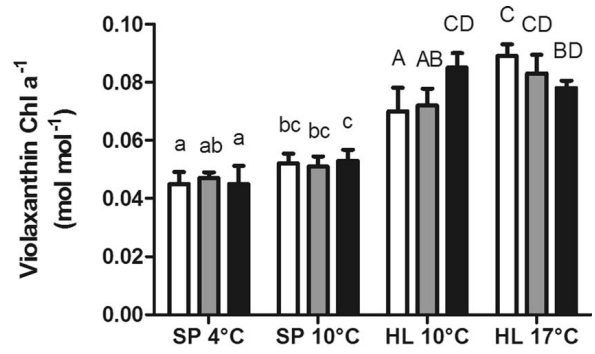
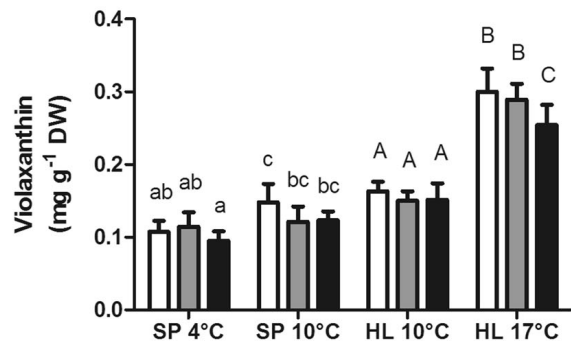
744

1 **Figures**



2

3 **Fig. 1** Effects of pCO₂ (white: present pCO₂; grey: expected future pCO₂; black: high pCO₂) and
 4 temperature on the accessory pigment content of *Saccharina latissima*, from Spitsbergen (SP) and
 5 Helgoland (HL). Different letters indicate significant differences. AP, accessory pigments



7 **Fig. 2** Effects of pCO₂ (white: present pCO₂; grey: expected future pCO₂; black: high pCO₂) and
 8 temperature on the xanthophyll-content of *Saccharina latissima*, from Spitsbergen (SP) and Helgoland
 9 (HL). Different letters indicate significant differences. VAZ, xanthophyll cycle pigment pool (sum of
 10 viola-, anthera- and zeaxanthin).

11

12

13

14

15

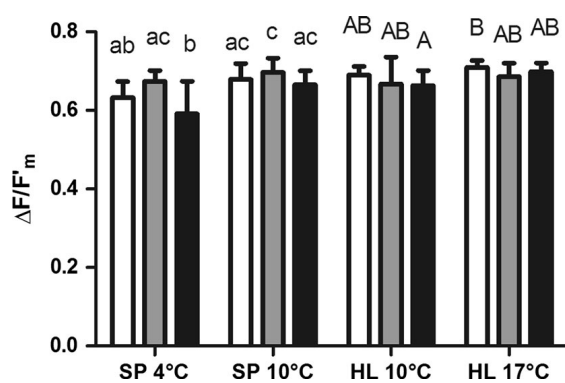
16

17

18

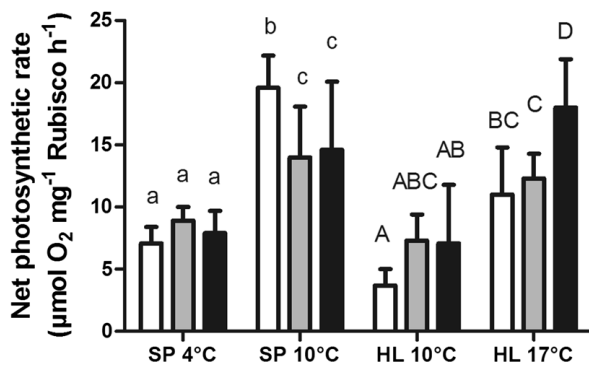
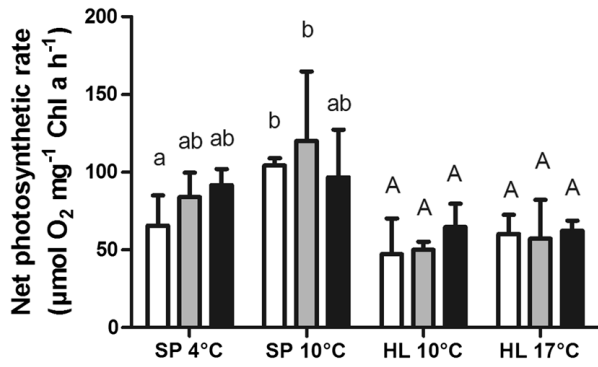
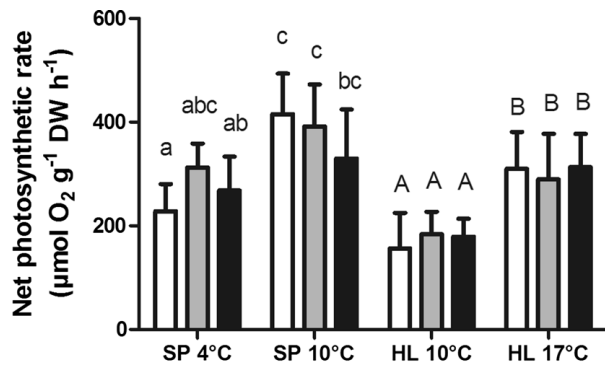
19

20



21

22 **Fig. 3** Effects of pCO₂ (white: present pCO₂; grey: expected future pCO₂; black: high pCO₂) and
 23 temperature on the $\Delta F/F_m$ ' of *Saccharina latissima*, from Spitsbergen (SP) and Helgoland (HL).
 24 Different letters indicate significant differences.



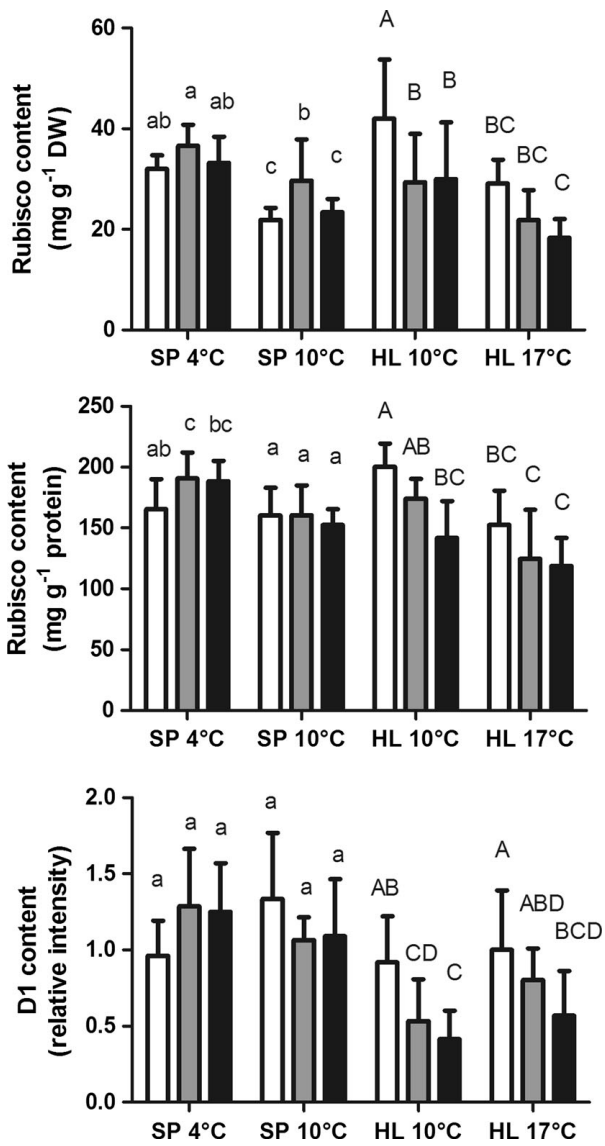
25

26 **Fig. 4** Effects of pCO₂ (white: present pCO₂; grey: expected future pCO₂; black: high pCO₂) and

27 temperature on the photosynthetic rate measured as O₂ evolution of *Saccharina latissima*, from

28 Spitsbergen (SP) and Helgoland (HL). Different letters indicate significant differences.

29



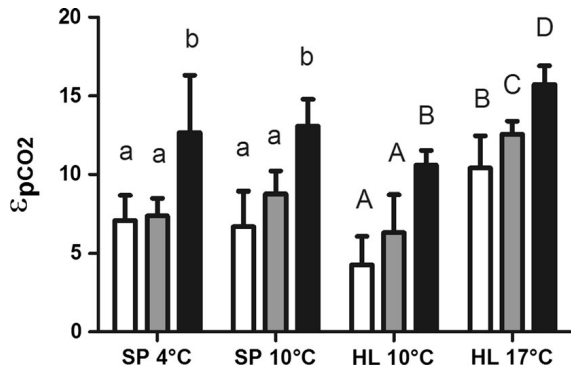
30

31 **Fig. 5** Effects of pCO₂ (white: present pCO₂; grey: expected future pCO₂; black: high pCO₂) and
 32 temperature on the Rubisco and D1 protein content of *Saccharina latissima*, from Spitsbergen (SP)
 33 and Helgoland (HL). Different letters indicate significant differences.

34

35

36



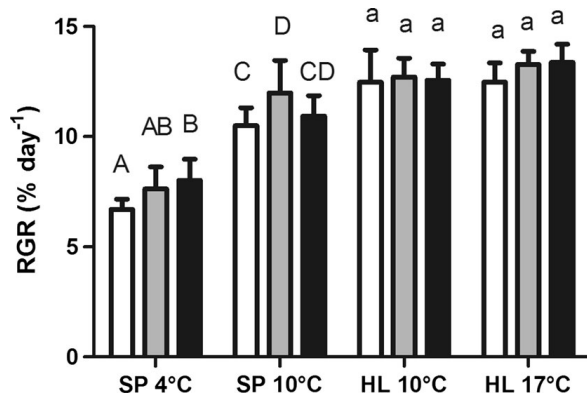
37

38 **Fig. 6** Effects of pCO₂ (white: present pCO₂; grey: expected future pCO₂; black: high pCO₂) and
 39 temperature on the ϵ_p values of *Saccharina latissima*, from Spitsbergen (SP) and Helgoland (HL).
 40 Different letters indicate significant differences.

41

42

43



44

45 **Fig. 7** Effects of pCO₂ (white: present pCO₂; grey: expected future pCO₂; black: high pCO₂) and
 46 temperature on the relative growth rate (RGR) in % day⁻¹ of *Saccharina latissima*, from Spitsbergen
 47 (SP) and Helgoland (HL). Different letters indicate significant differences.

Table 1 Results of the testing for significant influences of temperature, cultivation-pCO₂ and their interaction on the measured characteristics of *Saccharina latissima* from cold-temperate latitudes (Helgoland, HL, grey) and Spitsbergen (SP, white) by a two-way ANOVA. One asterisk indicates $P < 0.05$, two asterisks indicate $P < 0.01$ and three asterisks indicate $P < 0.001$.

Variable	Temperature	pCO ₂	Temperature * pCO ₂
Growth rate (HL)	n.s.	n.s.	n.s.
Growth rate (SP)	***	*	n.s.
Net photosynthesis (Chl <i>a</i> ⁻¹) (HL)	n.s.	n.s.	n.s.
Net photosynthesis (Chl <i>a</i> ⁻¹) (SP)	*	n.s.	n.s.
Net photosynthesis (DW ⁻¹) (HL)	***	n.s.	n.s.
Net photosynthesis (DW ⁻¹) (SP)	***	n.s.	n.s.
Net photosynthesis (mg ⁻¹ Rubisco) (HL)	***	*	n.s.
Net photosynthesis (mg ⁻¹ Rubisco) (SP)	***	n.s.	*
D1 protein (HL)	n.s.	**	n.s.
D1 Protein (SP)	n.s.	n.s.	n.s.
Rubisco (mg ⁻¹ proteins) (HL)	***	**	n.s.
Rubisco (mg ⁻¹ proteins) (SP)	**	n.s.	n.s.
Rubisco (mg ⁻¹ DW) (HL)	**	*	n.s.
Rubisco (mg ⁻¹ DW) (SP)	***	*	n.s.
ΔF/Fm' (HL)	n.s.	n.s.	n.s.
ΔF/Fm' (SP)	**	*	n.s.
Chl <i>a</i> (mg ⁻¹ DW) (HL)	***	n.s.	n.s.
Chl <i>a</i> (mg ⁻¹ DW) (SP)	n.s.	n.s.	n.s.
Chl <i>c</i> (mg ⁻¹ DW) (HL)	***	*	n.s.
Chl <i>c</i> (mg ⁻¹ DW) (SP)	n.s.	n.s.	n.s.
Fucoxanthin (mg ⁻¹ DW) (HL)	***	n.s.	n.s.
Fucoxanthin (mg ⁻¹ DW) (SP)	n.s.	n.s.	n.s.
Violaxanthin (mg ⁻¹ DW) (HL)	***	n.s.	n.s.
Violaxanthin (mg ⁻¹ DW) (SP)	**	n.s.	n.s.
Antheraxanthin (mg ⁻¹ DW) (HL)	n.s.	n.s.	n.s.
Antheraxanthin (mg ⁻¹ DW) (SP)	**	n.s.	n.s.
Zeaxanthin (mg ⁻¹ DW) (HL)	**	n.s.	n.s.
Zeaxanthin (mg ⁻¹ DW) (SP)	**	*	n.s.
β-carotene (mg ⁻¹ DW) (HL)	***	**	n.s.
β-carotene (mg ⁻¹ DW) (SP)	*	n.s.	n.s.
VAZ (mg ⁻¹ DW) (HL)	***	*	n.s.

VAZ (mg ⁻¹ DW) (SP)	n.s.	*	n.s.
DPS (HL)	***	n.s.	n.s.
DPS (SP)	***	n.s.	n.s.
ε _p (HL)	***	***	n.s.
ε _p (SP)	n.s.	***	n.s.

Table 2 Results of the testing for significant influences of temperature, cultivation-pCO₂ and their interaction on the pigment-content of *Saccharina latissima* relative to the Chl *a* from cold-temperate latitudes (Helgoland, HL, grey) and Spitsbergen (SP, white) by a two-way ANOVA. One asterisk indicates $P < 0.05$, two asterisks indicate $P < 0.01$ and three asterisks indicate $P < 0.001$.

Variable	Temperature	pCO ₂	Temperature * pCO ₂
Chl <i>c</i> Chl <i>a</i> ⁻¹ (mol mol ⁻¹) (HL)	n.s.	n.s.	n.s.
Chl <i>c</i> Chl <i>a</i> ⁻¹ (mol mol ⁻¹) (SP)	n.s.	n.s.	*
Fucoxanthin Chl <i>a</i> ⁻¹ (mol mol ⁻¹) (HL)	***	n.s.	n.s.
Fucoxanthin Chl <i>a</i> ⁻¹ (mol mol ⁻¹) (SP)	n.s.	n.s.	n.s.
β-carotene Chl <i>a</i> ⁻¹ (mol mol ⁻¹) (HL)	n.s.	n.s.	n.s.
β-carotene Chl <i>a</i> ⁻¹ (mol mol ⁻¹) (SP)	n.s.	n.s.	n.s.
Sum accessory pigments Chl <i>a</i> ⁻¹ (HL)	n.s.	n.s.	n.s.
Sum accessory pigments Chl <i>a</i> ⁻¹ (SP)	n.s.	n.s.	n.s.
Antheraxanthin Chl <i>a</i> ⁻¹ (mol mol ⁻¹) (HL)	***	n.s.	n.s.
Antheraxanthin Chl <i>a</i> ⁻¹ (mol mol ⁻¹) (SP)	***	n.s.	n.s.
Zeaxanthin Chl <i>a</i> ⁻¹ (mol mol ⁻¹) (HL)	***	n.s.	n.s.
Zeaxanthin Chl <i>a</i> ⁻¹ (mol mol ⁻¹) (SP)	***	*	n.s.
Violaxanthin Chl <i>a</i> ⁻¹ (mol mol ⁻¹) (HL)	**	n.s.	***
Violaxanthin Chl <i>a</i> ⁻¹ (mol mol ⁻¹) (SP)	***	n.s.	n.s.
VAZ Chl <i>a</i> ⁻¹ (mol mol ⁻¹) (HL)	***	n.s.	***
VAZ Chl <i>a</i> ⁻¹ (mol mol ⁻¹) (SP)	*	n.s.	n.s.

Table 3 Results of testing for significant differences in the measured characteristics between Arctic and cold-temperate populations of *Saccharina latissima* at 10°C (ecotypes) and the effects exerted by pCO₂ and its interaction with ecotype by a two-factorial ANOVA. One asterisk indicates $P < 0.05$, two asterisks indicate $P < 0.01$ and three asterisks indicate $P < 0.001$.

Variable	Ecotype	pCO ₂	Ecotype * pCO ₂
Growth rate	***	*	n.s.
Net photosynthesis (Chl a^{-1})	***	n.s.	n.s.
Net photosynthesis (DW ⁻¹)	***	n.s.	n.s.
Net photosynthesis (mg Rubisco ⁻¹)	***	n.s.	n.s.
D1 Protein	***	*	n.s.
Rubisco (mg proteins ⁻¹)	n.s.	*	n.s.
Rubisco (mg DW ⁻¹)	**	n.s.	*
$\Delta F/Fm'$	n.s.	n.s.	n.s.
Chl a (mg DW ⁻¹)	***	n.s.	n.s.
Chl c (mg DW ⁻¹)	n.s.	*	n.s.
Chl c Chl a^{-1} (mol mol ⁻¹)	***	n.s.	n.s.
Fucoxanthin (mg ⁻¹ DW)	n.s.	**	n.s.
Fucoxanthin Chl a^{-1} (mol mol ⁻¹)	***	n.s.	n.s.
Violaxanthin (mg ⁻¹ DW)	**	n.s.	n.s.
Violaxanthin Chl a^{-1} (mol mol ⁻¹)	***	*	*
Antheraxanthin (mg ⁻¹ DW)	***	n.s.	n.s.
Antheraxanthin Chl a^{-1} (mol mol ⁻¹)	***	n.s.	n.s.
Zeaxanthin (mg ⁻¹ DW)	n.s.	n.s.	n.s.
Zeaxanthin Chl a^{-1} (mol mol ⁻¹)	n.s.	n.s.	n.s.
β -carotene (mg ⁻¹ DW)	n.s.	**	n.s.
β -carotene Chl a^{-1} (mol mol ⁻¹)	***	n.s.	n.s.
Sum accessory pigments Chl a^{-1}	***	n.s.	n.s.
DPS	n.s.	n.s.	n.s.
VAZ (mg ⁻¹ DW)	***	*	n.s.
VAZ Chl a^{-1} (mol mol ⁻¹)	***	n.s.	n.s.
ϵ_p	***	***	n.s.

Supplements

List of supplements: Figure S1 (content of phlorotannins)

Supplement S1

The content of Phlorotannins was quantified as described in Olischläger et al. (2012)

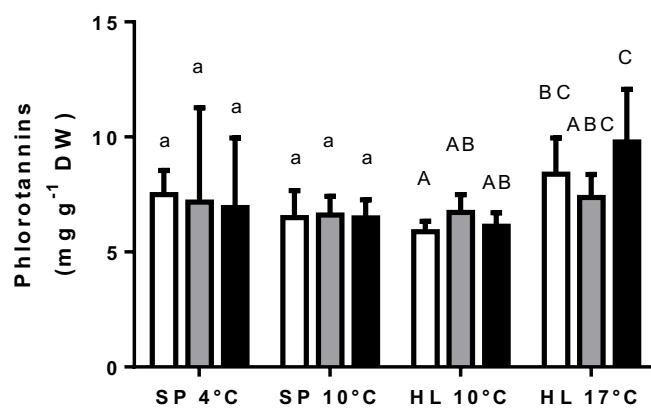


Figure S1: Content of phlorotannins (mean +SD) in *Saccharina latissima* macrothalli from cold-temperate latitudes (Helgoland, HL) and Spitsbergen (SP) after cultivation at present pCO₂ (white bar), expected future pCO₂ (gray bar) and high pCO₂ (black bar) at different temperatures.

